

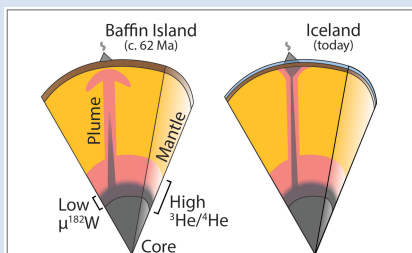
## Tungsten isotopes in Baffin Island lavas: Evidence of Iceland plume evolution

J. Kaare-Rasmussen<sup>1,2\*</sup>, D. Peters<sup>3</sup>, H. Rizo<sup>3</sup>, R.W. Carlson<sup>4</sup>, S.G. Nielsen<sup>2,5</sup>, F. Horton<sup>2</sup>



<https://doi.org/10.7185/geochemlet.2337>

### Abstract



$^{182}\text{W}/^{184}\text{W}$  anomalies. Over Earth history, tungsten diffusion from the core can explain the decline of  $^{182}\text{W}/^{184}\text{W}$  in the convecting mantle. We speculate that the uneven pace of this decline corresponds with evolving lower mantle dynamics.

Tungsten and helium isotope ratios in lavas derived from deeply rooted mantle plumes are tracers of lower mantle compositional heterogeneity or core–mantle exchange. We measured the tungsten isotopic compositions of lavas with exceptionally high  $^3\text{He}/^4\text{He}$  ratios that erupted above the head of the Iceland plume on Baffin Island. These lavas have  $^{182}\text{W}/^{184}\text{W}$  ratios that are indistinguishable from the convecting upper mantle, unlike younger lavas in Iceland that have lower  $^{182}\text{W}/^{184}\text{W}$  ratios. This implies that only the Iceland plume tail was infused with low- $^{182}\text{W}/^{184}\text{W}$  material, likely from the core. If high- $^3\text{He}/^4\text{He}$  helium also comes from the core, then diffusion across the core–mantle boundary may stratify plume-source mantle domains, with elevated  $^3\text{He}/^4\text{He}$  travelling farther into the lower mantle than

Received 17 May 2023 | Accepted 13 October 2023 | Published 8 November 2023

### Introduction

Geochemical heterogeneities preserved in Earth since its formation place fundamental constraints on planetary accretion and long-term evolution. Mantle plumes that sample the deepest portions of the mantle contain isotopic evidence of ancient, >4.5 Gyr, geochemical reservoirs that survived the mixing caused by giant impacts during the final stages of planetary accretion and billions of years of mantle convection (Mundl-Petermeier *et al.*, 2019). Two competing models have emerged that might explain the preservation of these ancient heterogeneities: (1) the preservation of ancient gas-rich mantle domains (*e.g.*, Kurz *et al.*, 1982) and (2) core–mantle chemical exchange since planetary accretion (*e.g.*, Rizo *et al.*, 2019). To test these hypotheses, we measured the tungsten (W) isotopic composition of Baffin Island lavas erupted above the Iceland mantle plume, which contains high- $^3\text{He}/^4\text{He}$  ratios that have been uniquely well preserved since planetary formation.

The  $^{182}\text{Hf}$ – $^{182}\text{W}$  isotope system is a sensitive tracer of core–mantle interaction. During the first ~60 Myr of solar system history,  $^{182}\text{W}$  was produced by the decay of the now extinct radionuclide  $^{182}\text{Hf}$  ( $t_{1/2} = 8.9$  Myr; Vockenhuber *et al.*, 2004). The upper terrestrial mantle has  $\mu^{182}\text{W} \approx 0$  (where  $\mu^{182}\text{W} = [(^{182}\text{W}/^{184}\text{W})_{\text{sample}} / (^{182}\text{W}/^{184}\text{W})_{\text{standard}} - 1] \times 10^6$ ), which is substantially higher than the average  $\mu^{182}\text{W}$  of chondrites of approximately  $-190$  (Kleine *et al.*, 2009). Because Hf is lithophile while W is moderately siderophile under reducing

conditions (*e.g.*, Wade *et al.*, 2013), core formation increased the Hf/W of the mantle and left the metallic core with Hf/W near zero. The superchondritic  $\mu^{182}\text{W}$  of the mantle thus most likely reflects core formation during the lifetime of  $^{182}\text{Hf}$ , in which case the core has  $\mu^{182}\text{W}$  lower than  $-190$ . Therefore, negative  $\mu^{182}\text{W}$  values observed in some mantle plume-related magmas may be evidence of core–mantle exchange (*e.g.*, Rizo *et al.*, 2019). Alternatively, the lowermost mantle could host ancient isotopic heterogeneities, either resulting from early silicate differentiation events (*e.g.*, Touboul *et al.*, 2012) or introduced during the late accretion of chondritic material with low  $\mu^{182}\text{W}$  relative to the terrestrial mantle (*e.g.*, Willbold *et al.*, 2011).

Intriguingly, some of the lowest  $\mu^{182}\text{W}$  values have been measured in lavas with elevated  $^3\text{He}/^4\text{He}$  compared to upper mantle values (greater than  $\sim 8$  Ra, where Ra is the atmospheric ratio; *e.g.*, Mundl-Petermeier *et al.*, 2020). This suggests that  $\mu^{182}\text{W}$  anomalies are associated with geochemical reservoirs that retain primordial  $^3\text{He}$  trapped during planetary accretion before nebular gases dispersed, or  $^3\text{He}$  that was accreted later from solar wind irradiated meteoritic material (Mukhopadhyay and Parai, 2019). Traditionally, high  $^3\text{He}/^4\text{He}$  has been attributed to the preservation of primordial mantle domains, either in the entire lower mantle (*e.g.*, Kurz *et al.*, 1982) or within certain regions in the lower mantle (*e.g.*, Rizo *et al.*, 2016). Alternatively, high- $^3\text{He}/^4\text{He}$  helium concentrated in the core might escape and become entrained in mantle plumes (Bouhifd *et al.*, 2013). If so, core–mantle exchange may explain the observation that

1. The MIT-WHOI Joint Program in Oceanography/Applied Ocean Science and Engineering, Woods Hole, MA 02543, USA  
 2. Department of Geology and Geophysics, Woods Hole Oceanographic Institution, Woods Hole, MA 02543, USA  
 3. Department of Earth Sciences, Carleton University, Ottawa-Carleton Geoscience Centre, Ottawa, ON K1S 5B6, Canada  
 4. Earth & Planets Laboratory, Carnegie Institution for Science, Washington, DC 20015, USA  
 5. NIRVANA Laboratories, Woods Hole Oceanographic Institution, Woods Hole, MA 02543, USA

\* Corresponding author (Email: [jkaaras@mit.edu](mailto:jkaaras@mit.edu))



high- $^3\text{He}/^4\text{He}$  ratios correlate with low  $\mu^{182}\text{W}$  in some mantle plumes (Mundl-Petermeier *et al.*, 2019, 2020). As more data become available, however, the correlation between W and He isotopic compositions in modern ocean island basalts (OIBs) seems less universal.

Lavas erupted at c. 62 Ma on Baffin Island above the Iceland mantle plume have the highest  $^3\text{He}/^4\text{He}$  of any measured terrestrial igneous rock (Horton *et al.*, 2023) and therefore contain an unusually pure primordial helium component. Thus, if high  $^3\text{He}/^4\text{He}$  is sourced from the core, it might reasonably be expected that these lavas also exhibit low  $\mu^{182}\text{W}$ . In this study, we reassess  $\mu^{182}\text{W}$  in high- $^3\text{He}/^4\text{He}$  lavas from Baffin Island because previous attempts to measure their W isotopic compositions have produced inconsistent results (Rizo *et al.*, 2016; Jansen *et al.*, 2022).

## Results

We analysed glass picked from five Baffin Island pillow lavas containing olivine phenocrysts. Tungsten concentrations (20.9–107.0 ng g $^{-1}$ ) correlate with other highly incompatible and immobile elements, such as Th, but do not vary systematically with Sr, Nd, or Hf isotopic compositions (Fig. S-4). Weighted average  $\mu^{182}\text{W}$  and  $\mu^{183}\text{W}$  are  $-2.7 \pm 6.6$  and  $+2.8 \pm 6.6$ , respectively (2 s.d.,  $n = 5$ ; Table 1, Fig. 1). All  $\mu^{182}\text{W}$  and  $\mu^{183}\text{W}$  from individual samples are indistinguishable at the 2 s.e. confidence level from the Alfa Aesar and NIST SRM 3163 standards (Table S-1, Fig. S-5).

The lack of resolvable  $\mu^{182}\text{W}$  anomalies in Baffin Island lavas agrees with the results published by Jansen *et al.* (2022) and from the stratigraphically similar lavas from West Greenland (Mundl-Petermeier *et al.*, 2019) but differs from the

positive  $\mu^{182}\text{W}$  anomalies reported by Rizo *et al.* (2016). Improvements in N-TIMS techniques, including the ability to quantify the oxygen isotopic compositions during tungsten oxide measurements (see Supplementary Information), give us confidence that these results are more representative of the Baffin Island mantle source than results published in Rizo *et al.* (2016), which should be interpreted with caution. Also, the absence of  $\mu^{183}\text{W}$  anomalies in data reported here alleviates concerns raised by the Jansen *et al.* (2022) dataset about contamination and mass-independent fractionation.

The helium isotopic compositions of Baffin Island lavas are well characterised (*e.g.*, Horton *et al.*, 2023; Table S-2) and have been reported for two samples analysed in this study: olivine crushing experiments for RB18-H3 and PING18-H2 imply minimum magmatic  $^3\text{He}/^4\text{He}$  ratios of  $36.8 \pm 2.0$  and  $55.1 \pm 1.3$  Ra, respectively (Horton *et al.*, 2023). Olivine separates from the remaining three samples yielded insufficient helium for isotopic characterisation. These samples contained smaller olivines (<1 mm) than the helium-rich samples (>3 mm); we suspect that the low helium contents of the former reflect olivine growth after magma degassing. Nonetheless, the  $\mu^{182}\text{W}$  results reported here are unambiguously associated with high- $^3\text{He}/^4\text{He}$  lavas.

## Discussion

*The origins of the tungsten and helium in the Iceland plume.* Our  $\mu^{182}\text{W}$  results are unresolvable from the mantle and therefore do not require a core component in Baffin Island lavas source. Yet, the high- $^3\text{He}/^4\text{He}$  helium and solar-like neon (Horton *et al.*, 2023) in these rocks and other lavas from the Iceland plume have presumably been preserved in Earth since the late stages of planetary accretion. On a global scale, rock samples from all 15 hotspots with anomalously low  $\mu^{182}\text{W}$  also have anomalously high  $^3\text{He}/^4\text{He}$  (Mundl-Petermeier *et al.*, 2020). This suggests a common origin of both elements in mantle plumes, such as primordial or ancient mantle, late accreted material, or the core.

Given the high W concentrations and positive  $\mu^{182}\text{W}$  of Archean crust, small amounts of crustal assimilation could mask a core  $\mu^{182}\text{W}$  signature. Assimilation modelling (see Supplementary Information) predicts correlations between  $\mu^{182}\text{W}$ , trace elements, and long-lived radiogenic isotope ratios that are not observed in our data. This suggests that crustal assimilation is unlikely to have significantly influenced the W isotopic compositions of the Baffin Island lavas. Rather, the lack of  $\mu^{182}\text{W}$  anomalies in Baffin Island high- $^3\text{He}/^4\text{He}$  lavas indicates that helium and tungsten in plumes either (a) derive from a common source but are decoupled in the Iceland plume, or (b) have different origins. Either way, plumes

**Table 1** Tungsten isotopic compositions of the Baffin Island samples.  $\mu^{182}\text{W}$  and  $\mu^{183}\text{W}$  are reported as deviations from the Alfa Aesar standard ( $^{182}\text{W}/^{184}\text{W} = 0.864888 \pm 0.000006$  and  $^{183}\text{W}/^{184}\text{W} = 0.467151 \pm 0.000004$ , 2 s.e.,  $n = 8$ ) and normalised to  $^{186}\text{W}/^{184}\text{W}$ , denoted by subscript 6/4. 2 s.e. represents the internal run precision of each individual analyses.

Sample	$\mu^{182}\text{W}_{6/4}$	2 s.e.	$\mu^{183}\text{W}_{6/4}$	2 s.e.
PING18-H16	-7.3	5.0	-0.6	4.5
PING18-H2	-0.6	4.2	2.2	3.5
PING18-H20	0.5	3.8	6.9	3.3
DURB18-H11	-1.7	6.0	4.3	5.1
RB18-H3	-5.3	4.8	-0.8	3.9

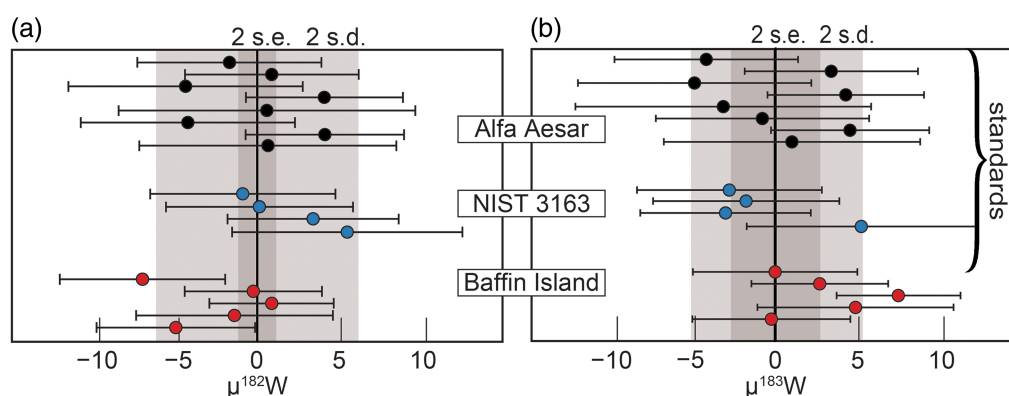


**Figure 1** (a)  $\mu^{182}\text{W}$  and (b)  $\mu^{183}\text{W}$  for Alfa Aesar standard, NIST 3163 standard, and Baffin Island lavas.

appear to form in ways that produce systematic He-W correlations in many cases, but not universally.

The hypothesis that the high- $^3\text{He}/^4\text{He}$  ratios are derived from primordial, non-degassed mantle in the Baffin Island lavas is inconsistent with other geochemical constraints, including our new  $\mu^{182}\text{W}$  data. The primordial mantle likely had positive  $\mu^{182}\text{W}$ , based on the positive  $\mu^{182}\text{W}$  compositions of the Moon (Kruijer *et al.*, 2012; Touboul *et al.*, 2015) and mantle-derived rocks in the Archean (e.g., Reimink *et al.*, 2020, and references therein). However, modern mantle plumes do not have positive  $\mu^{182}\text{W}$ . Furthermore, the Baffin Island lavas have superchondritic  $^{143}\text{Nd}/^{144}\text{Nd}$  and  $^{176}\text{Hf}/^{177}\text{Hf}$  (Willhite *et al.*, 2019), suggesting they are not derived from a primordial mantle component but a differentiated mantle reservoir. These observations, combined with correlations between high  $^3\text{He}/^4\text{He}$  and low  $\mu^{182}\text{W}$  in many hotspots globally, imply the latter likely derive from a common deep Earth reservoir that is not primordial mantle.

Ancient differentiated mantle reservoirs that formed while  $^{182}\text{Hf}$  was extant are similarly difficult to reconcile with coupled He-W isotopic compositions. Magma ocean silicate cumulates generated in the aftermath of the Moon-forming giant impact should be depleted in incompatible trace elements and might host high- $^3\text{He}/^4\text{He}$  helium (Coltice *et al.*, 2011). If formed while  $^{182}\text{Hf}$  was extant, cumulates would presumably acquire a positive  $\mu^{182}\text{W}$  composition because W is more incompatible than Hf in silicate minerals (Righter and Shearer, 2003). Therefore, an ancient depleted mantle with high  $^3\text{He}/^4\text{He}$  would be expected to have higher  $\mu^{182}\text{W}$  than primordial mantle. Furthermore, silicate differentiation would have fractionated Sm from Nd, thereby influencing the abundances of  $^{142}\text{Nd}$ —the product of  $^{146}\text{Sm}$  decay ( $t_{1/2} \approx 100$  Myr)—in the segregates. However, like most post-Archean mantle-derived rocks, Baffin Island (de Leeuw *et al.*, 2017) and Iceland lavas (Murphy *et al.*, 2010) lack  $^{142}\text{Nd}/^{144}\text{Nd}$  anomalies. This indicates that the Iceland plume did not derive from mantle differentiated during the lifetimes of  $^{146}\text{Sm}$  or  $^{182}\text{Hf}$ .

Silicate differentiation within Hadean crust might have produced restite with low  $\mu^{182}\text{W}$  decoupled from  $^{142}\text{Nd}/^{144}\text{Nd}$  (Tusch *et al.*, 2022). However, the formation of, and subsequent magmatic differentiation within, Hadean crust would have caused extensive degassing of primordial gases. If so, Hadean crustal restites that foundered into the mantle would acquire

low  $^3\text{He}/^4\text{He}$  over time. Mantle plumes incorporating such material would acquire positively correlated  $^3\text{He}/^4\text{He}$  and  $\mu^{182}\text{W}$ , which is not observed.

Alternatively, hidden low- $\mu^{182}\text{W}$  mantle domains—perhaps formed during late accretion—are potential hosts of primordial  $^3\text{He}$ . The  $\mu^{182}\text{W}$  of the convecting mantle may have decreased by  $\sim 27$  since Moon formation, based on lunar and Eoarchean terrestrial rock compositions (e.g., Willbold *et al.*, 2011). About 0.5 wt. % of late accreting chondritic material with high W and highly siderophile element (HSE) concentrations but low  $\mu^{182}\text{W}$  might explain the decline in mantle  $\mu^{182}\text{W}$  (Willbold *et al.*, 2011). Mantle domains that contain an above average amount of late accreting material have been proposed as alternative sources of negative  $\mu^{182}\text{W}$  (Marchi *et al.*, 2018). However, late accretion seems an unlikely common source of W and He because most late accreting material is expected to have high  $^3\text{He}/^4\text{He}$  and to be HSE-rich, yet high- $^3\text{He}/^4\text{He}$  helium in late accreting materials would not necessarily enter the mantle, and HSE abundances do not correlate with  $\mu^{182}\text{W}$  or  $^3\text{He}/^4\text{He}$  in mantle plumes (e.g., Rizo *et al.*, 2019). Although estimating the mantle source HSE abundances from the HSE contents of erupted magmas is difficult, to our knowledge, no clear correlation between  $\mu^{182}\text{W}$  and the HSE content has been demonstrated in spite of the wide range in  $\mu^{182}\text{W}$  seen in OIBs.

Given the above discussion, combined with W isotope evidence from other mantle plumes, the negative  $\mu^{182}\text{W}$  anomalies (as low as  $-12.9$ ) in some Iceland high- $^3\text{He}/^4\text{He}$  lavas might derive from the core (Mundl-Petermeier *et al.*, 2019). Even though the Baffin Island lavas do not have a  $\mu^{182}\text{W}$  anomaly outside the analytical uncertainty, the external reproducibility of these samples still allow a small amount of bulk core material ( $\sim 1.08\%$ ) mixed with ambient mid-ocean ridge basalt (MORB)-like depleted mantle (see Supplementary Information, Fig. S-6). However, bulk mixing of this much core into the mantle is mechanically improbable and inconsistent with the Os concentrations in Iceland and Baffin Island lavas (Rizo *et al.*, 2016; Mundl-Petermeier *et al.*, 2019), which limit the amount of bulk core contribution to  $<0.1\%$ , assuming  $2.83 \mu\text{g g}^{-1}$  Os in the core (Day, 2013).

Importantly,  $^3\text{He}/^4\text{He}$  appears decoupled from not only W but also from lithophile elements, HSEs, and heavier noble gases in the Iceland plume (e.g., Mundl-Petermeier *et al.*, 2019). This observation is consistent with helium diffusion into Iceland

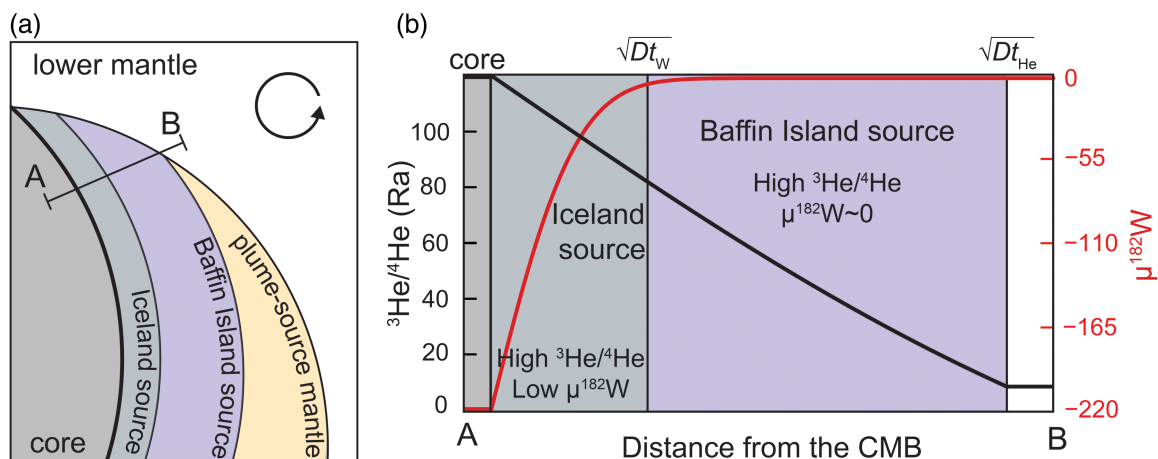


**Figure 2** Conceptual model of a stratified Iceland plume source region. (a) On Gyr timescales, diffusion across the CMB may lower  $\mu^{182}\text{W}$  and raise  $^3\text{He}/^4\text{He}$  in the lowermost mantle on different length scales. (b) In such a scenario, there would be isotopic gradients in the lowermost mantle from the core ( $\mu^{182}\text{W} = -200$ ,  $^3\text{He}/^4\text{He} = 120$  Ra) to ambient mantle ( $\mu^{182}\text{W} = 0$ ,  $^3\text{He}/^4\text{He} = 8$  Ra). Iceland and Baffin Island mantle sources may derive from within and beyond the region impacted by W isotopic diffusion, respectively. Calculations for the isotopic composition curves are in the Supplementary Information and assume a diffusion timescale of 1 Gyr.



mantle from—rather than bulk mixing with—a  $^3\text{He}$ -rich reservoir. Theoretically, He concentration gradients (Horton *et al.*, 2023) and W isotopic gradients (Ferrick and Korenaga, 2023) exist across the core–mantle boundary (CMB) that could drive diffusion into the mantle (Fig. 2). Alternatively, He and W diffused into the Iceland plume source from different reservoirs, such as ancient differentiated mantle and the core, respectively.

Helium may diffuse farther into mantle plume sources than W. Assuming the mantle plume source is stable on Gyr timescales (as expected for large low-shear wave velocity provinces, LLSVPs; *e.g.*, Ferrick and Korenaga, 2023), the characteristic length scales of diffusion ( $\sqrt{Dt}$ ) for helium might be  $\sim 40$  km, if theoretical diffusion rates for the upper mantle (Wang *et al.*, 2015) are extrapolated to lower mantle temperatures. For W, this length scale may be only 5–10 km (Ferrick and Korenaga, 2023), suggesting that mantle domains farther from the CMB may be characterised by He but not W isotopic anomalies. If anomalous W and He in the Iceland plume diffused from the core, our results imply that the plume head originated farther from the CMB than the plume tail.

Baffin Island mantle may have originated from the periphery of a helium-infused zone in the lowermost mantle (10–40 km from the core), whereas low- $\mu^{182}\text{W}$  Iceland mantle might have resided nearer the core (Fig. 2). Negative  $\mu^{182}\text{W}$  anomalies may only exist in the Iceland plume tail, which may have preferentially entrained denser material proximal to the core–mantle boundary (Jones *et al.*, 2019). The plume head, from which Baffin Island lavas derived, may have instead entrained primarily portions of the lowermost mantle beyond the diffusion limit of W but still infused with  $^3\text{He}$  from the core. Thus, plume tails might be the most efficient conveyors of material from the CMB.

This model predicts that  $^3\text{He}/^4\text{He}$  is highest in lavas with the most negative  $\mu^{182}\text{W}$ , a trend observed for all high- $^3\text{He}/^4\text{He}$  hotspots, except the Iceland plume (Jackson *et al.*, 2020). Maximum  $^3\text{He}/^4\text{He}$  in Iceland plume lavas apparently declined from  $>65$  Ra at 62 Ma (Horton *et al.*, 2023) to  $<26$  Ra in the neovolcanic zones of Iceland (Harðardóttir *et al.*, 2018). This decline could be due to the incorporation of convecting upper mantle into the Iceland plume—enough to explain up to a 40 % MORB component in modern Iceland lavas—as a result of the ridge-centred plume position (Shorttle and MacLennan, 2011). The addition of this much material from the convecting upper mantle would have moderated  $^3\text{He}/^4\text{He}$  and  $\mu^{182}\text{W}$ , implying that the Iceland plume itself currently exhibits  $\mu^{182}\text{W}$  closer to  $-21$ .

**Implications for planetary accretion and convecting mantle evolution.** By combining  $\mu^{142}\text{Nd}$  and  $\mu^{182}\text{W}$  constraints with our diffusion model, an early Earth chronology emerges. Some Eoarchean rocks have  $^{142}\text{Nd}$  anomalies (*e.g.*, Caro *et al.*, 2003) produced by igneous differentiation that fractionated Sm and Nd prior to 4 Ga. Such differentiation could be expected to also fractionate Hf from W, so any differentiation that occurred before  $^{182}\text{Hf}$  became extinct would have produced  $\mu^{182}\text{W}$  anomalies that would correlate with  $\mu^{142}\text{Nd}$  variations (Touboul *et al.*, 2012). However, correlations between  $\mu^{142}\text{Nd}$  and  $\mu^{182}\text{W}$  are rarely observed. Instead, these observations seem consistent with: (i) a Moon-forming impact after  $^{182}\text{Hf}$  was extinct ( $\sim 4.5$  Ga) that homogenised the silicate portions of the Earth–Moon system, (ii) generation of  $^{142}\text{Nd}/^{144}\text{Nd}$  anomalies in the mantle by differentiation events that post-dated the Moon-forming impact that were subsequently erased by mixing after the extinction of  $^{146}\text{Sm}$  around 4 Ga, and (iii)  $\mu^{182}\text{W}$  decline in the mantle until present caused by CMB diffusion.

The inferred mantle  $\mu^{182}\text{W}$  decline since the Hadean requires that the average residence time ( $\tau$ ) of material diffused

from the core at the CMB was  $\leq 30$  Myr (Fig. 3a). Due to the higher temperatures in early Earth, early mantle convection may have been rapid. Fast convection would also have efficiently homogenised the mantle and, hence, efficient W isotopic transfer across the CMB (Hadean rapid convection path, Fig. 3b). However,  $\mu^{142}\text{Nd}$  and positive  $\mu^{182}\text{W}$  heterogeneities throughout the mantle persisted at least until the end of the Archean, and potentially even for longer (Slowing mantle convection path, Fig. 3b). Perhaps the  $\mu^{182}\text{W}$  of the mantle rapidly decreased during the late Archean to early Proterozoic, coinciding with development of continents and therefore a liminal stage of mantle dynamics. Alternatively, CMB cover by long-term stable structures may have increased in the late Archean (*i.e.* increasing  $\xi$ ), inhibiting transfer of core-derived W to the convecting mantle. Either way, this transition suggests a link between continent formation and lower mantle dynamics during the initiation of modern plate tectonics.

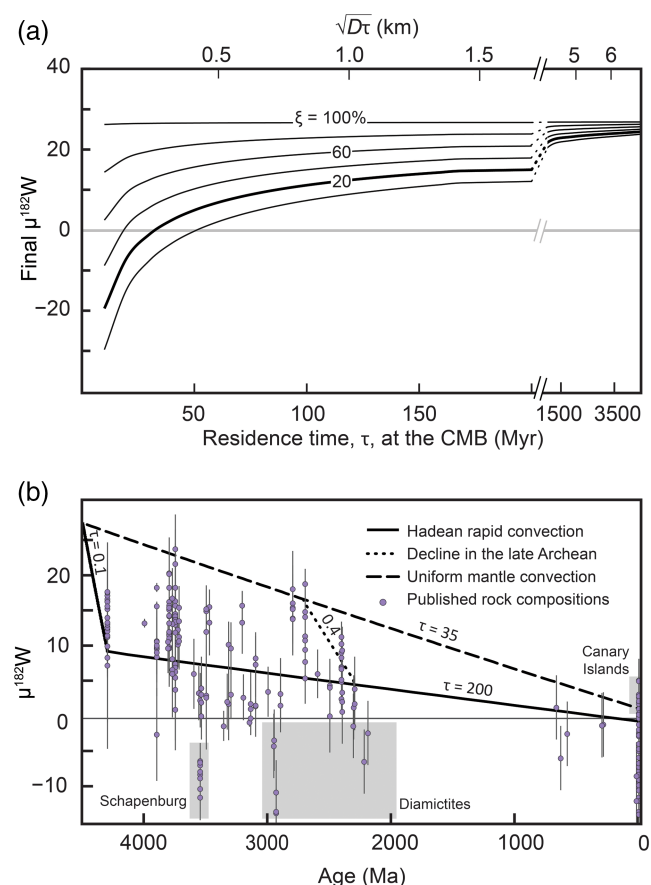


**Figure 3** (a) Modern mantle  $\mu^{182}\text{W}$  may be a function of the mantle residence time,  $\tau$ , at the CMB and the percentage of the core surface area,  $\xi$ , insulated by long-term stable structures. We assume that (i) the early mantle had  $\mu^{182}\text{W}$  of the Moon (+27); (ii) basal mantle acquired core-like  $\mu^{182}\text{W}$  corresponding to the characteristic length scale of diffusion ( $\sqrt{Dt}$ ), where  $D$  is the diffusivity ( $D = 4.62 \times 10^{-10} \text{ m}^2 \text{ s}^{-1}$ ; Ferrick and Korenaga, 2023); and (iii) core-infused mantle parcels mixed efficiently into the bulk mantle. Diffusion can explain a  $\mu^{182}\text{W}$  decline to zero if  $\tau$  is short ( $< 30$  Myr) and the CMB is  $< 20\%$  insulated. (b) A compilation of  $\mu^{182}\text{W}$  data (Reimink *et al.*, 2020; Nakanishi *et al.*, 2023) and three potential mantle  $\mu^{182}\text{W}$  trajectories: (i) constant  $\tau = 35$  Myr; (ii) fast Hadean decline ( $\tau = 0.1$  Myr) corresponding to rapid Hadean convection followed by slower decline ( $\tau = 200$  Myr); and (iii) fast early Paleoproterozoic decline ( $\tau = 0.4$  Myr) due to a change in the style of plate tectonics.



## Acknowledgements

We thank M. Mahy of Parks Canada Nunavut Field Unit for assisting with fieldwork planning and Shuangquan Zhang at the IGGRC of Carleton University for technical support. This work was funded by a National Science Foundation grant awarded to F. Horton (NSF EAR-1911699), a Natural Sciences and Engineering Research Council of Canada Discovery Grant awarded to H. Rizo (RGPIN-477144-2015), and an Ontario Early Researcher Award received by H. Rizo. Additional support came from a National Science Foundation grant awarded to S.G. Nielsen (EAR-1829546), the Woods Hole Oceanographic Institution Andrew W. Mellon Foundation Endowed Fund for Innovative Research, and a National Geographic Society grant (CP4-144R-18), which supported fieldwork activities. Comments from two anonymous reviewers and editor Raul O.C. Fonseca improved this manuscript.

Editor: Raúl Fonseca

## Additional Information

Supplementary Information accompanies this letter at <https://www.geochemicalperspectivesletters.org/article2337>.



© 2023 The Authors. This work is distributed under the Creative Commons Attribution Non-Commercial No-Derivatives 4.0

License, which permits unrestricted distribution provided the original author and source are credited. The material may not be adapted (remixed, transformed or built upon) or used for commercial purposes without written permission from the author. Additional information is available at <https://www.geochemicalperspectivesletters.org/copyright-and-permissions>.

Cite this letter as: Kaare-Rasmussen, J., Peters, D., Rizo, H., Carlson, R.W., Nielsen, S.G., Horton, F. (2023) Tungsten isotopes in Baffin Island lavas: Evidence of Iceland plume evolution. *Geochem. Persp. Let.* 28, 7–12. <https://doi.org/10.7185/geochemlet.2337>

## References

- BOUHIFED, M.A., JEPHCOAT, A.P., HEBER, V.S., KELLEY, S.P. (2013) Helium in Earth's early core. *Nature Geoscience* 6, 982–986. <https://doi.org/10.1038/ngeo1959>
- CARO, G., BOURDON, B., BIRCK, J.-L., MOORBATH, S. (2003)  $^{146}\text{Sm}$ – $^{142}\text{Nd}$  evidence from Isua metamorphosed sediments for early differentiation of the Earth's mantle. *Nature* 423, 428–432. <https://doi.org/10.1038/nature01668>
- COLTICE, N., MOREIRA, M., HERNLUND, J., LABROSSE, S. (2011) Crystallization of a basal magma ocean recorded by Helium and Neon. *Earth and Planetary Science Letters* 308, 193–199. <https://doi.org/10.1016/j.epsl.2011.05.045>
- DAY, J.M.D. (2013) Hotspot volcanism and highly siderophile elements. *Chemical Geology* 341, 50–74. <https://doi.org/10.1016/j.chemgeo.2012.12.010>
- DE LEEUW, G.A.M., ELLAM, R.M., STUART, F.M., CARLSON, R.W. (2017)  $^{142}\text{Nd}/^{144}\text{Nd}$  inferences on the nature and origin of the source of high  $^3\text{He}/^4\text{He}$  magmas. *Earth and Planetary Science Letters* 472, 62–68. <https://doi.org/10.1016/j.epsl.2017.05.005>
- FERRICK, A.L., KORENAGA, J. (2023) Long-term core–mantle interaction explains W–He isotope heterogeneities. *Proceedings of the National Academy of Sciences* 120, e2215903120. <https://doi.org/10.1073/pnas.2215903120>
- HARDARDÓTTIR, S., HALLDÓRSSON, S.A., HILTON, D.R. (2018) Spatial distribution of helium isotopes in Icelandic geothermal fluids and volcanic materials with implications for location, upwelling and evolution of the Icelandic mantle plume. *Chemical Geology* 480, 12–27. <https://doi.org/10.1016/j.chemgeo.2017.05.012>
- HORTON, F., ASIMOW, P.D., FARLEY, K.A., CURTICE, J., KURZ, M.D., BLUSZTAIN, J., BIASI, J., BOYES, X.M. (2023) Highest terrestrial  $^3\text{He}/^4\text{He}$  credibly from the core. *Nature* 623, 90–94. <https://doi.org/10.1038/s41586-023-06590-8>
- JACKSON, M.G., Blichert-Toft, J., HALLDÓRSSON, S.A., MUNDL-PETERMEIER, A., BIZIMIS, M., KURZ, M.D., PRICE, A.A., HARDARDÓTTIR, S., WILLHITE, L.N., BEDDAM, K., BECKER, T.W., FISCHER, R.A. (2020) Ancient helium and tungsten isotopic signatures preserved in mantle domains least modified by crustal recycling. *Proceedings of the National Academy of Sciences* 117, 30993–31001. <https://doi.org/10.1073/pnas.2009663117>
- JANSEN, M.W., TUSCH, J., MÜNCKER, C., BRAGAGNI, A., AVANZINELLI, R., MASTROIANNI, F., STUART, F.M., KURZWEIL, F. (2022) Upper mantle control on the W isotope record of shallow level plume and intraplate volcanic settings. *Earth and Planetary Science Letters* 585, 117507. <https://doi.org/10.1016/j.epsl.2022.117507>
- JONES, T.D., DAVIES, D.R., SOSSI, P.A. (2019) Tungsten isotopes in mantle plumes: Heads it's positive, tails it's negative. *Earth and Planetary Science Letters* 506, 255–267. <https://doi.org/10.1016/j.epsl.2018.11.008>
- KLEINE, T., TOUBOUL, M., BOURDON, B., NIMMO, F., MEZGER, K., PALME, H., JACOBSEN, S.B., YIN, Q.-Z., HALLIDAY, A.N. (2009) Hf–W chronology of the accretion and early evolution of asteroids and terrestrial planets. *Geochimica et Cosmochimica Acta* 73, 5150–5188. <https://doi.org/10.1016/j.gca.2008.11.047>
- KRUIJER, T.S., SPRUNG, P., KLEINE, T., LEYA, I., BURKHARDT, C., WIELER, R. (2012) Hf–W chronometry of core formation in planetesimals inferred from weakly irradiated iron meteorites. *Geochimica et Cosmochimica Acta* 99, 287–304. <https://doi.org/10.1016/j.gca.2012.09.015>
- KURZ, M.D., JENKINS, W.J., HART, S.R. (1982) Helium isotopic systematics of oceanic islands and mantle heterogeneity. *Nature* 297, 43–47. <https://doi.org/10.1038/297043a0>
- MARCHI, S., CANUP, R.M., WALKER, R.J. (2018) Heterogeneous delivery of silicate and metal to the Earth by large planetesimals. *Nature Geoscience* 11, 77–81. <https://doi.org/10.1038/s41561-017-0022-3>
- MUKHOPADHYAY, S., PARAL, R. (2019) Noble Gases: A Record of Earth's Evolution and Mantle Dynamics. *Annual Review of Earth and Planetary Sciences* 47, 389–419. <https://doi.org/10.1146/annurev-earth-053018-060238>
- MUNDL-PETERMEIER, A., WALKER, R.J., JACKSON, M.G., Blichert-Toft, J., KURZ, M.D., HALLDÓRSSON, S.A. (2019) Temporal evolution of primordial tungsten-182 and  $^3\text{He}/^4\text{He}$  signatures in the Iceland mantle plume. *Chemical Geology* 525, 245–259. <https://doi.org/10.1016/j.chemgeo.2019.07.026>
- MUNDL-PETERMEIER, A., WALKER, R.J., FISCHER, R.A., LEKIC, V., JACKSON, M.G., KURZ, M.D. (2020) Anomalous  $^{182}\text{W}$  in high  $^3\text{He}/^4\text{He}$  ocean island basalts: Fingerprints of Earth's core? *Geochimica et Cosmochimica Acta* 271, 194–211. <https://doi.org/10.1016/j.gca.2019.12.020>
- MURPHY, D.T., BRANDON, A.D., DEBAILLE, V., BURGESS, R., BALLENTINE, C. (2010) In search of a hidden long-term isolated sub-chondritic  $^{142}\text{Nd}/^{144}\text{Nd}$  reservoir in the deep mantle: Implications for the Nd isotope systematics of the Earth. *Geochimica et Cosmochimica Acta* 74, 738–750. <https://doi.org/10.1016/j.gca.2009.10.005>
- NAKANISHI, N., PUCHTEL, I.S., WALKER, R.J., NABELEK, P.I. (2023) Dissipation of Tungsten-182 Anomalies in the Archean Upper Mantle: Evidence from the Black Hills, South Dakota, USA. *Chemical Geology* 617, 121255. <https://doi.org/10.1016/j.chemgeo.2022.121255>
- REIMINK, J.R., MUNDL-PETERMEIER, A., CARLSON, R.W., SHIREY, S.B., WALKER, R.J., PEARSON, D.G. (2020) Tungsten Isotope Composition of Archean Crustal Reservoirs and Implications for Terrestrial  $\mu^{182}\text{W}$  Evolution. *Geochemistry, Geophysics, Geosystems* 21, e2020GC009155. <https://doi.org/10.1029/2020GC009155>
- RIGHTER, K., SHEARER, C.K. (2003) Magmatic fractionation of Hf and W: constraints on the timing of core formation and differentiation in the Moon and Mars. *Geochimica et Cosmochimica Acta* 67, 2497–2507. [https://doi.org/10.1016/S0016-7037\(02\)01349-2](https://doi.org/10.1016/S0016-7037(02)01349-2)
- RIZO, H., WALKER, R.J., CARLSON, R.W., HORAN, M.F., MUKHOPADHYAY, S., MANTHOS, V., FRANCIS, D., JACKSON, M.G. (2016) Preservation of Earth-forming events in the tungsten isotopic composition of modern flood basalts. *Science* 352, 809–812. <https://doi.org/10.1126/science.aad8563>
- RIZO, H., ANDRAULT, D., BENNETT, N.R., HUMAYUN, M., BRANDON, A., VLASTELIC, I., MOINE, B., POIRIER, A., BOUHIFED, M.A., MURPHY, D.T. (2019)  $^{182}\text{W}$  evidence for core–mantle interaction in the source of mantle plumes. *Geochemical Perspectives Letters* 11, 6–11. <https://doi.org/10.7185/geochemlet.1917>
- SHORTILE, O., MACLENNAN, J. (2011) Compositional trends of Icelandic basalts: Implications for short-length scale lithological heterogeneity in mantle plumes. *Geochemistry, Geophysics, Geosystems* 12, Q11008. <https://doi.org/10.1029/2011GC003748>
- TOUBOUL, M., PUCHTEL, I.S., WALKER, R.J. (2012)  $^{182}\text{W}$  Evidence for Long-Term Preservation of Early Mantle Differentiation Products. *Science* 335, 1065–1069. <https://doi.org/10.1126/science.1216351>
- TOUBOUL, M., PUCHTEL, I.S., WALKER, R.J. (2015) Tungsten isotopic evidence for disproportional late accretion to the Earth and Moon. *Nature* 520, 530–533. <https://doi.org/10.1038/nature14355>



- TUSCH, J., HOFFMANN, J.E., HASENSTAB, E., FISCHER-GÖDDE, M., MARIEN, C.S., WILSON, A.H., MÜNKER, C. (2022) Long-term preservation of Hadean protocrust in Earth's mantle. *Proceedings of the National Academy of Sciences* 119, e2120241119. <https://doi.org/10.1073/pnas.2120241119>
- VOCKENHUBER, C., BICHLER, M., GOLSER, R., KUTSCHERA, W., PRILLER, A., STEIER, P., WINKLER, S. (2004)  $^{182}\text{Hf}$ , a new isotope for AMS. *Nuclear Instruments and Methods in Physics Research Section B: Beam Interactions with Materials and Atoms* 223–224, 823–828. <https://doi.org/10.1016/j.nimb.2004.04.152>
- WADE, J., WOOD, B.J., NORRIS, C.A. (2013) The oxidation state of tungsten in silicate melt at high pressures and temperatures. *Chemical Geology* 335, 189–193. <https://doi.org/10.1016/j.chemgeo.2012.10.011>
- WANG, K., BRODHOLT, J., LU, X. (2015) Helium diffusion in olivine from first principles calculations. *Geochimica et Cosmochimica Acta* 156, 145–153. <https://doi.org/10.1016/j.gca.2015.01.023>
- WILLBOLD, M., ELLIOTT, T., MOORBATH, S. (2011) The tungsten isotopic composition of the Earth's mantle before the terminal bombardment. *Nature* 477, 195–198. <https://doi.org/10.1038/nature10399>
- WILLHITE, L.N., JACKSON, M.G., Blichert-Toft, J., BINDEMAN, I., KURZ, M.D., HALLDÓRSSON, S.A., HARDARDÓTTIR, S., GAZEL, E., PRICE, A.A., BYERLY, B.L. (2019) Hot and Heterogenous High- $^3\text{He}/^4\text{He}$  Components: New Constraints From Proto-Iceland Plume Lavas From Baffin Island. *Geochemistry, Geophysics, Geosystems* 20, 5939–5967. <https://doi.org/10.1029/2019GC008654>

# Tungsten isotopes in Baffin Island lavas: Evidence of Iceland plume evolution

J. Kaare-Rasmussen, D. Peters, H. Rizo, R.W. Carlson,  
S.G. Nielsen, F. Horton

## Supplementary Information

The Supplementary Information includes:

- 1. Analytical Methods
- 2. Methodology Developments
- 3. Crustal Contamination
- 4. Calculating Diffusion in the Long-term Stable Mantle Plume Source
- 5. Diffusion Calculations in the Convecting Mantle
- Tables S-1 and S-2
- Figures S-1 to S-6
- Supplementary Information References

### 1. Analytical Methods

Glassy pillow rinds were cut from samples using a diamond-bit rock saw. Sawn surfaces were sanded away using silica-carbide-grit paper to remove any metal contamination from the saw. Samples were then crushed using metal-free tools (rubber mallets, ceramic mortar and pestle) to avoid metal contamination. Under a binocular microscope, 11.54–12.36 g of clean glass chips were picked by hand to avoid palagonite. Samples were then dissolved in new, clean, Savillex Teflon beakers using a mixture of ultrapure (pg g<sup>-1</sup>-level) concentrated HF-HNO<sub>3</sub> reagents, followed by repeated dry downs and redissolutions in concentrated HNO<sub>3</sub>. Finally, samples were dried down and dissolved in 6 M HCl.

A ~5 % mass aliquot was separated from the samples in 6 M HCl solution to analyse W concentrations *via* isotope dilution. Sample aliquots (~0.5 g total) were spiked with a <sup>186</sup>W tracer, dried down, and re-



dissolved to achieve sample-spike equilibrium. Tungsten was isolated using ion chromatography as described in Nagai and Yokoyama (2014). Tungsten concentration measurements were performed using the ThermoFisher Neptune multicollector ICP-MS at the Department of Earth Sciences of Carleton University (Ottawa, Canada).

For high-precision isotope ratio analyses, W was separated from the remaining non-spiked 95 % aliquots using three column steps. The first column, filled with 20 mL of AG50W-X8 (200–400 mesh) resin, separated W and other high field strength elements (HFSE) from the rock matrix in a procedure similar to that described in Touboul and Walker (2012). The second column, filled with 10 mL of AG1-X8 (200–400 mesh) resin, separated W from other HFSEs, as well as any remaining Ti and Al, as described in Breton and Quitté (2014). Finally, the samples passed through a third clean-up column with 0.3 mL AG1-X8 (200–400 mesh) to remove any remaining Ti, which can hinder W ionisation efficiency (Touboul and Walker, 2012). Purified W solutions were redissolved with a drop of concentrated HNO<sub>3</sub>-HCl-H<sub>2</sub>O<sub>2</sub> several times in open Savillex beakers at 150 °C before being redissolved in 0.5 N HCl – 0.5 N HF and loaded onto single degassed zone-refined rhenium filaments. Tungsten blanks were <4 ng and yields were greater than ~50 %.

Tungsten isotopes were measured as WO<sub>3</sub><sup>-</sup> anions on the ThermoFisher Triton thermal ionisation mass spectrometer (TIMS) at the Department of Earth Sciences of Carleton University (Ottawa, Canada). Loaded W amounts were 346–1323 ng for the unknowns. Tungsten oxides were produced and ionised using a La-Gd activator solution and O<sub>2</sub> bled into the TIMS source at a source pressure of approximately  $1.15 \times 10^{-7}$  mbar. Tungsten isotopes were measured using a protocol similar to the one described in Archer *et al.* (2017), in which dominant oxides (*e.g.*, W<sup>16</sup>O<sub>3</sub><sup>-</sup>) were measured on Faraday cups connected to 10<sup>11</sup> Ω amplifiers. Trace oxides, such as <sup>186</sup>W<sup>16</sup>O<sub>2</sub><sup>18</sup>O<sup>-</sup>, were measured with Faraday cups coupled to 10<sup>12</sup> Ω amplifiers. Measurements were performed using a multistatic method with three steps, during which <sup>184</sup>WO<sub>3</sub>, <sup>185</sup>ReO<sub>3</sub> and <sup>186</sup>WO<sub>3</sub> were sequentially measured with the axial detector. Step 1 had an integration time of 33 s and an idle time of 12 s to allow for low-noise measurements of <sup>186</sup>W<sup>16</sup>O<sub>2</sub><sup>18</sup>O<sup>-</sup> and <sup>187</sup>Re<sup>16</sup>O<sub>2</sub><sup>18</sup>O<sup>-</sup> using a 10<sup>12</sup> Ω amplifier. Acquisition



cycles 2 and 3 did not measure the trace oxides and therefore had a collection time of 8 s and an idle time of 4 s. Individual W isotope analyses contain 173–640 cycles (averaging 400 cycles per analysis), divided into 20-cycle blocks. Throughout the analytical session, 1200 s baselines were obtained every 7 blocks. Peak centring and lens focusing were repeated every 3 blocks to minimise drift. Steps 1 and 2 were averaged to calculate mean  $^{182}\text{W}/^{184}\text{W}$  and  $^{183}\text{W}/^{184}\text{W}$  ratios. All W isotopic ratios have been corrected for instrumental fractionation using the  $^{186}\text{W}/^{184}\text{W}$  ratio of 0.92767 (Völkening *et al.*, 1991) and O isotopic compositional relations from Archer *et al.* (2017). Results are reported in  $\mu$ -notation relative to the Alfa Aesar W reference material. The weighted mean isotopic composition of 500 ng and 1000 ng aliquots the Alfa Aesar reference material was  $^{182}\text{W}/^{184}\text{W} = 0.864888 \pm 0.000006$  (2 s.e.,  $n = 8$ ) and  $^{183}\text{W}/^{184}\text{W} = 0.467151 \pm 0.000004$  (2 s.e.,  $n = 8$ ).

To assess measurement accuracy and repeatability, 500 ng aliquots of the National Institute of Standards and Technology (NIST) W isotope standard solution 3163 was repeatedly measured throughout the analytical session. Normalised to the Alfa Aesar reference material, NIST 3163 yielded  $\mu^{182}\text{W} = +2.0 \pm 5.8$  (2 s.d.,  $n = 4$ ) and  $\mu^{183}\text{W} = -0.6 \pm 7.7$  (2 s.d.,  $n = 4$ ), which agree with literature values (Kruijer *et al.*, 2012).

## 2. Methodology Developments

Rizo *et al.* (2016) reported  $\mu^{182}\text{W}$  excesses ranging from +10 to +48 in Baffin Island lavas. This section discusses the acquisition methodology of Touboul and Walker (2012) and speculates about causes for the discrepancy between the results of Rizo *et al.* (2016) and this study.

Rizo *et al.* (2016) utilised the W isotope measurement techniques outlined in Touboul and Walker (2012), which involve N-TIMS analyses of  $\text{WO}_3^-$  species using Faraday collectors equipped with  $10^{11} \Omega$  amplifiers. The measured W isotopic ratios were corrected for instrumental mass fractionation using the  $^{186}\text{W}/^{184}\text{W}$  ratio. The fractionation-corrected  $^{182}\text{W}/^{184}\text{W}$  and  $^{183}\text{W}/^{184}\text{W}$  exhibit residual positive correlations that were attributed to mass-dependent fractionation of oxygen isotopes (Touboul and Walker, 2012). To



determine the  $^{182}\text{W}/^{184}\text{W}$  ratio, a second-order correction was necessary using an assumed natural  $^{183}\text{W}/^{184}\text{W}$  ratio of 0.467151 (Fig. S-1).

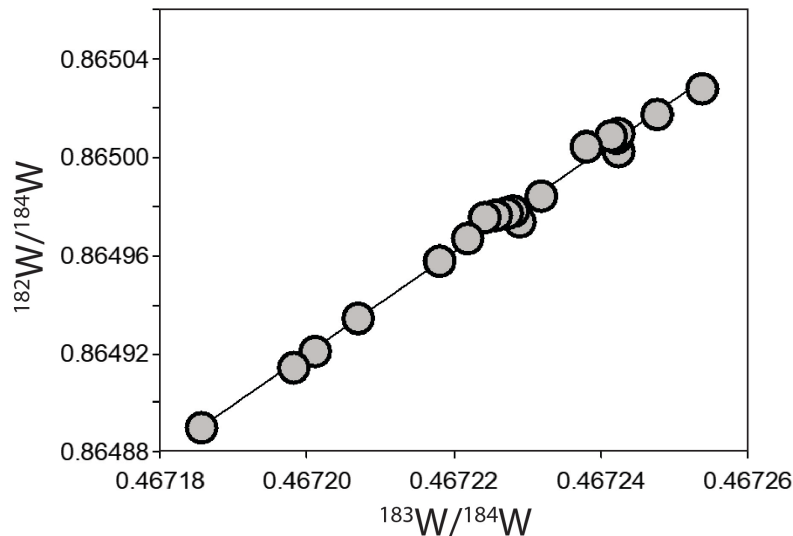


**Figure S-1** Explanatory diagram of  $^{182}\text{W}/^{184}\text{W}$  and  $^{183}\text{W}/^{184}\text{W}$  illustrating how  $^{182}\text{W}/^{184}\text{W}$  ratios were determined in Rizo *et al.* (2016). Correlated  $^{182}\text{W}/^{184}\text{W}$  and  $^{183}\text{W}/^{184}\text{W}$  ratios of W standards were obtained after instrumental mass fractionation using the  $^{186}\text{W}/^{184}\text{W}$  ratio. The final  $^{182}\text{W}/^{184}\text{W}$  was obtained by assuming a natural  $^{183}\text{W}/^{184}\text{W}$  ratio of 0.467151.

N-TIMS methodology for W isotope ratio determinations improved when Archer *et al.* (2017) developed a procedure for measuring the oxygen isotopic composition of  $\text{WO}_3^-$  molecules. This involved equipping two Faraday detectors with  $10^{12} \Omega$  amplifiers, which enabled measurements of low abundance W oxides (*e.g.*,  $^{186}\text{W}^{16}\text{O}_2^{18}\text{O}$  ion beams are typically  $\sim 5$  mV). By measuring, for example,  $^{186}\text{W}^{16}\text{O}_3$  and  $^{186}\text{W}^{16}\text{O}_2^{18}\text{O}$  molecules, precise measurements of oxygen isotopic compositions can be obtained (Fig. S-2). This permits a correction for oxygen isotopic fractionation during the analysis and thereby eliminates the need



for a second-order W isotopic correction. As a result, direct measurement of  $^{183}\text{W}/^{184}\text{W}$  became possible with a similar level of precision as  $^{182}\text{W}/^{184}\text{W}$ .

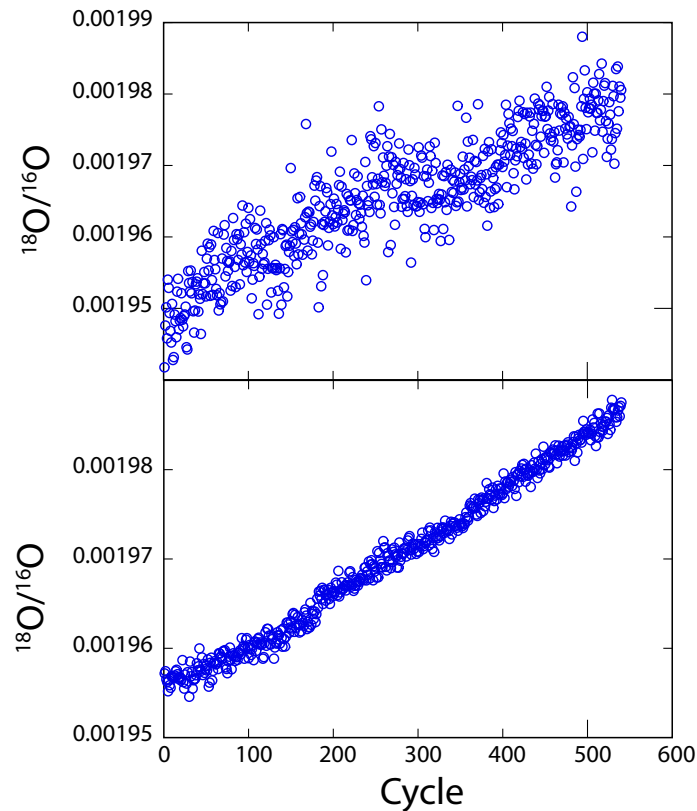


**Figure S-2** Oxygen isotopic compositions change during individual analyses. (Top) The oxygen isotopic evolution during measurements of a standard using standard  $10^{11} \Omega$  amplifiers. (Bottom) The same as above but with  $10^{12} \Omega$  amplifiers, which amplify the signal/noise ratio by a factor of 3.

The  $^{182}\text{W}$  excesses reported by Rizo *et al.* (2016) have been attributed to nuclear field shift effects (*e.g.*, Kruijer and Kleine, 2018). However, analysis of Baffin Island lavas with improved N-TIMS methods indicates that these rocks lack  $^{183}\text{W}/^{184}\text{W}$  anomalies, which is inconsistent with nuclear field shifts. Evidence of nuclear

field shifts has not emerged from the growing dataset produced using the same N-TIMS methodology (Archer *et al.*, 2017; Mundl *et al.*, 2017; Rizo *et al.*, 2019; Mundl-Petermeier *et al.*, 2020; Nakanishi *et al.*, 2023).

The source of  $^{182}\text{W}$  excesses reported by Rizo *et al.* (2016) remains uncertain. Contamination from a  $^{186}\text{W}$  spike may have produced high  $^{182}\text{W}/^{184}\text{W}$  ratios. Reducing Rizo *et al.* (2016) data for sample Pd-2 using  $^{183}\text{W}/^{184}\text{W}$  for fractionation correction instead of  $^{186}\text{W}/^{184}\text{W}$  yields a  $\mu^{182}\text{W}$  of  $-14$  and a  $\mu^{186}\text{W}$  of  $+146$ , which may be consistent with spike contamination. Mixing as little as 7 pg of W from the  $^{186}\text{W}$  spike into that sample could have produced the high  $\mu^{186}\text{W}$  value. Alternatively, an atypical oxygen isotopic composition during the analysis may have caused artificially high  $^{182}\text{W}/^{184}\text{W}$  measurements. Assuming sample Pd-2 had  $\mu^{182}\text{W} \approx 0$ , the  $\delta^{18}\text{O}$  of the sample would have been 20–27 ‰ lighter than the Nier values of the standards. If so, inaccurate oxygen isotopic corrections can explain the  $\mu^{182}\text{W}$  excesses. In any case, the improved N-TIMS methodology employed in this study overcomes previous limitations and more accurately constrains Baffin Island lava  $\mu^{182}\text{W}$ .

### 3. Crustal Contamination

Continental crust assimilation may affect the  $\mu^{182}\text{W}$  compositions of lavas. Tungsten is incompatible during mantle melting and is therefore enriched in continental crust relative to the mantle. Thus, assimilated continental crust could dominate the W budget of a mafic magma and overprint intrinsic  $\mu^{182}\text{W}$  anomalies. This is especially true for Archean crust with positive  $\mu^{182}\text{W}$  anomalies that might mask any core-derived  $\mu^{182}\text{W}$  signature (Reimink *et al.*, 2020, and references therein). In this case, the observation of negative  $\mu^{182}\text{W}$  in Iceland but not Baffin Island lavas might reflect the masking of a negative  $\mu^{182}\text{W}$  plume component by assimilated crust in the Baffin Island only.

The Baffin Island lavas erupted through the southeastern margin of the Rae Craton (St-Onge *et al.*, 2009, 2020). Variability in radiogenic isotopes (Sr, Nd and Pb) and trace element ratios (Nb/Th, Ce/Pb) implies the Baffin Island lavas and conjugate western Greenland lavas assimilated variable amounts of



continental crust (Larsen and Pedersen, 2009; Willhite *et al.*, 2019). Willhite *et al.* (2019) showed that the Baffin Island lavas with the most radiogenic  $^{143}\text{Nd}/^{144}\text{Nd}$  and least radiogenic  $^{87}\text{Sr}/^{86}\text{Sr}$  ratios in the Baffin Island lava suite did not experience significant assimilation of crustal material. Using a range of crustal compositions, they were unable to simultaneously replicate the whole rock radiogenic isotope compositions and trace element ratios in two component mixing between crustal compositions and the primitive magmas erupting in the modern Iceland plume. Their work provides useful geochemical context for placing bounds on the extent of crustal contamination in the Baffin Island lavas analysed for W isotopes.

Whereas most radiogenic  $^{143}\text{Nd}/^{144}\text{Nd}$  and least radiogenic  $^{87}\text{Sr}/^{86}\text{Sr}$  ratios measured in the Baffin Island lavas may approximate the composition of the primary magmas ( $^{87}\text{Sr}/^{86}\text{Sr} = 0.702995$  and  $^{143}\text{Nd}/^{144}\text{Nd} = 0.513174$ ; Willhite *et al.*, 2019), their Nd and Sr concentrations—dependent on the extent of melting and fractional crystallisation—are uncertain. We assume a lower limit ( $[\text{Sr}] = 7.664 \mu\text{g g}^{-1}$  and  $[\text{Nd}] = 0.581 \mu\text{g g}^{-1}$ ; Workman and Hart, 2005) equal to depleted MORB mantle (DMM) and an upper limit equal to the least-contaminated Baffin Island lavas ( $[\text{Sr}] = 48.9 \mu\text{g g}^{-1}$  and  $[\text{Nd}] = 2.42 \mu\text{g g}^{-1}$ ; Willhite *et al.*, 2019). We further assume that the assimilated crust had a composition similar to Precambrian shales in western Greenland (sample 113450,  $[\text{Sr}] = 192.81 \mu\text{g g}^{-1}$ ,  $[\text{Nd}] = 47.931 \mu\text{g g}^{-1}$ ,  $^{87}\text{Sr}/^{86}\text{Sr} = 0.721081$ , and  $^{143}\text{Nd}/^{144}\text{Nd} = 0.5111164$ ; Larsen and Pedersen, 2009). Based on our lower and upper limits for primary magma  $[\text{Nd}]$  and  $[\text{Sr}]$ ,  $^{143}\text{Nd}/^{144}\text{Nd}$  and  $^{87}\text{Sr}/^{86}\text{Sr}$  variability in our dataset can be explained by  $\leq 0.2\%$  or  $\leq 1\%$  crustal assimilation, respectively.

The sensitivity of magmas to  $\mu^{182}\text{W}$  overprinting depends on the composition of the primary magmas, as well as the crust. A  $\mu^{182}\text{W}$  anomaly of the same magnitude as those measured in Iceland ( $-12.6$ ; Mundl-Petermeier *et al.*, 2019) can be fully overprinted by the assimilation of 6% crust with  $\mu^{182}\text{W} = 0$  or 0.65% Archean crust with  $\mu^{182}\text{W} = +20$ , assuming that the assimilated crust has W concentrations equal to average upper continental crust ( $1.9 \mu\text{g g}^{-1}$ ; Rudnick and Gao, 2003). If the Sr and Nd isotope systematics only allow for at most 0.2% crustal assimilation, then even Archean crust cannot overprint a  $\mu^{182}\text{W}$  anomaly of  $-12.6$ .





However, 1 % Archean crust assimilation could entirely mask this  $\mu^{182}\text{W}$  composition. Better constraints for Baffin Island basement are necessary to further constrain the potential overprinting effects. Therefore, we cannot rule out the possibility that the Baffin Island mantle source contains negative  $\mu^{182}\text{W}$  anomalies that were overprinted during crustal assimilation.

Nonetheless, the lack of correlation among elemental and isotopic ratios in Baffin Island lavas implies that W isotopic overprinting in our samples is unlikely. Willhite *et al.* (2019) proposed a series of filters for crustal assimilation in Baffin Island lavas. They propose that samples with  $>10$  wt.% MgO, Nb/Th  $> 13$  and Ce/Pb  $> 20$  have minimal crustal contamination. Only one of our samples fit into the least-contaminated sample set, based on these criteria (RB18-H3); the rest pass at least one of the three filters. If  $\mu^{182}\text{W}$  is a function of crustal assimilation, we would expect to see correlation between  $\mu^{182}\text{W}$  and other assimilation tracers (*e.g.*, MgO, Ce/Pb, Nb/Th, or  $^{87}\text{Sr}/^{86}\text{Sr}$  and  $^{143}\text{Nd}/^{144}\text{Nd}$  ratios) because our samples contain evidence for variable degrees of crustal assimilation. Importantly, within our sample set there is no correlation between  $\mu^{182}\text{W}$  and crustal assimilation tracers such as MgO, Ce/Pb, Nb/Th, or  $^{87}\text{Sr}/^{86}\text{Sr}$  and  $^{143}\text{Nd}/^{144}\text{Nd}$  ratios. Thus, although it is possible the  $\mu^{182}\text{W}$  we report for Baffin Island lavas is the result of crustal assimilation, it would require the basement rocks to have a positive  $\mu^{182}\text{W}$  anomaly or much more crustal assimilation ( $\sim 6$  %) than the radiogenic isotopes and trace element ratios permit. More likely, the  $\mu^{182}\text{W}$  reported here is representative of the mantle plume.

#### 4. Calculating Diffusion in the Long-term Stable Mantle Plume Source

Isotopic diffusion across the CMB is a function of the isotopic compositions of the core ( $c_c$ ) and mantle ( $c_m$ ), time ( $t$ ), and diffusivity ( $D$ ). Isotopic diffusion can be approximated using Fick's second law as  $\frac{\partial c}{\partial t} = D \frac{\partial^2 c}{\partial x^2}$ , where  $x$  is the distance from the core. Under the assumption that the core and mantle are infinite isotopic reservoirs, a one-dimensional concentration gradient across the core-mantle boundary can be calculated from



the general solution of Fick's second law as  $c(x, t) = c_c - (c_c - c_m)\text{erf}\left(\frac{x}{2\sqrt{Dt}}\right)$ . The error function ( $\text{erf}[z]$ ) is calculated by  $\text{erf}(z) = \frac{2}{\sqrt{\pi}} \int_0^z e^{-t^2} dt$ . Fick's second law predicts the diffusion gradient changes with time. Therefore, we use a constant time (1 Gyr) to calculate  $c(x, 1 \text{ Gyr})$  for  $x$  along the length of stable structures at the CMB, where  $c_{(c, W)} = -200$  (e.g., Rizo *et al.*, 2019),  $c_{(m, W)} = 0$ ,  $c_{(c, He)} = 120 \text{ Ra}$  (e.g., Atreya *et al.*, 2003),  $c_{(m, He)} = 8 \text{ Ra}$  (e.g., Moreira and Kurz, 2013). The diffusivities of W and He are poorly constrained. Under the assumption that diffusivities are not pressure dependent,  $D_W$  and  $D_{He}$  were extrapolated from experimentally determined diffusivities at standard temperature and pressure ( $D_W = 4.62 \times 10^{-10} \text{ m}^2 \text{ s}^{-1}$  and  $D_{He} = 10^{-10} \text{ m}^2 \text{ s}^{-1}$ ; Hart *et al.*, 2008; Yoshino *et al.*, 2020; Ferrick and Korenaga, 2023) using the Arrhenius equation  $D = D_0 e^{-E_A/RT}$ , where  $D_0$  is the diffusivity,  $E_A$  is the activation energy,  $T$  is the temperature at the core-mantle boundary (4000 K), and  $R$  is the gas constant. Tungsten volume diffusion is expected to be negligible (e.g., Yoshino *et al.*, 2020), so we consider  $D_{W,0}$  as solely grain boundary diffusion calculated using the assumptions in Ferrick and Korenaga (2023). Helium volume diffusion in olivine is relatively slow and offers a good lower bound for the diffusivity of He, which we use for  $D_{He,0}$  after Hart *et al.* (2008). Nevertheless, this exercise demonstrates that He and W might be mobile over large enough regions in the lowermost mantle to influence plumes that originate near the CMB, and that He and W might be kinetically fractionated. This model suggests that core-like  $^3\text{He}/^4\text{He}$  can be transported farther from the CMB than negative  $\mu^{182}\text{W}$  anomalies, but the diffusion limits for He and W are so uncertain that we plot distance from the CMB as unitless in Figure 2.

## 5. Diffusion Calculations in the Convecting Mantle

The diffusion of W from the core into the mantle might explain the inferred  $\mu^{182}\text{W}$  decline of  $\sim 27$  in the convecting mantle. Mantle  $\mu^{182}\text{W}$  evolution is dependent on the timescales of convecting mantle residence on the CMB (residence time,  $\tau$ ) and the percentage of the CMB that is insulated by long-term stable structures ( $\xi$ ). We envisage a scenario in which conveyor belts of convecting mantle are in contact with the core, except



where stable structures exist, and that the isotopic anomalies acquired *via* diffusion from the core are efficiently mixed into the rest of the convecting mantle (*i.e.*, the entire mantle minus the long-term structures at the CMB). We first calculate how many unique parcels of convecting mantle were exposed to the core by dividing the duration of mantle convection (assumed to be 4.5 Gyr) by  $\tau$ . For example, if  $\tau = 100$ , there have been 45 unique parcels of mantle on the CMB. Next, we calculate the volume of the convecting mantle into which core-like  $\mu^{182}\text{W}$  diffused. To do this, we multiply the CMB area exposed to the convecting mantle (the surface area of the core  $\times \xi$ ) by the characteristic diffusion length scale ( $\sqrt{D\tau}$  where  $D$  is diffusivity). We assume that (a) this volume acquired core-like  $\mu^{182}\text{W}$  during its residence at the CMB (*e.g.*, Ferrick and Korenaga, 2023) and (b) it mixes efficiently into the convecting mantle. After each unique parcel cycle, we calculate the average convecting mantle  $\mu^{182}\text{W}$ .

Convection rates in the ancient mantle are a major source of uncertainty for this model. Giant impacts, the rise of modern plate tectonics, and secular cooling of the mantle likely influenced convection rates. Therefore, we calculated different paths through mantle  $\mu^{182}\text{W}$ -time space with varying mantle convection rates. A first-order question is what  $\tau$  can fully explain the  $\sim 27$  decrease in average mantle  $\mu^{182}\text{W}$ . We modelled a constant decrease in average mantle  $\mu^{182}\text{W}$  using  $\tau = 35$  Myr in the dashed line (Fig. 3b). Such a quick refresh rate can explain the mantle decrease through time; however, this does not fit the published Archean data well. Ferrick and Korenaga (2023) assumed that  $\tau \approx 100$  Myr in the modern Earth, but poor constraints exist for this value. We also modelled two other end-member cases, one where there is a steep decrease in a rapidly convecting mantle early in Earth history ( $\tau = 0.1$  Myr) in a whole mantle magma ocean scenario. Then a constant  $\tau = 200$  Myr.  $\tau$  is expected to increase as the mantle cools. Gradual cooling might lead to a gradual increase in  $\tau$ , which fits the lower bound of published Archean data well. Finally, there is evidence for a sharp change in  $\mu^{182}\text{W}$  near the end of the Archean (*e.g.*, Nakanishi *et al.*, 2023). This may be emblematic of the initiation of modern plate tectonics, which we model with a sharp decrease in  $\mu^{182}\text{W}$  around 3 Ga ( $\tau = 0.4$  Myr). This path (dotted line in Fig. 3b) fits the upper end of published Archean  $\mu^{182}\text{W}$  data.



## Supplementary Tables

**Table S-1** Isotopic compositions of the standards. Both  $\mu^{182}\text{W}$  and  $\mu^{183}\text{W}$  are reported as  $\mu\text{g g}^{-1}$  deviations from the average Alfa Aesar standard ( $^{182}\text{W}/^{184}\text{W} = 0.864888 \pm 0.000006$  and  $^{183}\text{W}/^{184}\text{W} = 0.467151 \pm 0.000004$ , 2 s.e.,  $n = 8$ ), respectively. Both  $\mu^{182}\text{W}$  and  $\mu^{183}\text{W}$  are normalised to  $^{186}\text{W}/^{184}\text{W}$ , denoted by subscript 6/4. The internal run precision of each individual analyses is reported as 2 s.e.

Sample	$\mu^{182}\text{W}_{6/4}$	2 s.e.	$\mu^{183}\text{W}_{6/4}$	2 s.e.
Alfa Aesar 1-4	-2.0	5.6	-4.8	4.5
Alfa Aesar 1-5	0.5	5.3	2.9	4.4
Alfa Aesar 1-6	-4.7	7.1	-5.5	6.3
Alfa Aesar 2-2	0.3	7.8	0.5	6.1
Alfa Aesar 2-3	0.2	9.0	-3.7	8.1
Alfa Aesar 2-5	-4.6	6.5	-1.3	5.9
Alfa Aesar 3-4	3.7	4.8	4.0	4.2
Alfa Aesar 3-5	3.7	4.8	3.7	4.1
NIST 3163-1	5.1	7.0	4.7	6.4
NIST 3163-2	-0.2	5.7	-2.3	5.1
NIST 3163-3	3.0	5.2	-3.6	4.7
NIST 3163-4	-1.2	5.6	-3.3	4.7

**Table S-2** Elemental concentration from the Baffin Island lavas. Starred samples produced usable  $\mu^{182}\text{W}$  data. Helium isotopic compositions are the highest reproducible ratios from Horton *et al.* (2023), normalised to the atmospheric ratio of  $1.384 \times 10^{-6}$  (Ra).

Sample	[W] (ng g <sup>-1</sup> )	[Th] (ng g <sup>-1</sup> )	[U] (ng g <sup>-1</sup> )	<sup>3</sup> He/ <sup>4</sup> He (Ra)	2 s.e.
DURB18-H4	21.8	93.4	23.3	-	-
DURB18-H11*	20.9	91.3	24.2	39.0	3.5
PING18-H2*	107.0	443.0	102.3	65.9	3.4
PING18-H3	30.9	118.3	31.9	43.9	1.4
PING18-H16*	90.6	105.0	71.4	-	-
PING18-H19	78.6	325.9	58.7	-	-
PING18-H20*	85.3	302.2	70.0	-	-
RB18-H3*	26.2	292.8	34.1	36.3	8.9



## Supplementary Figures

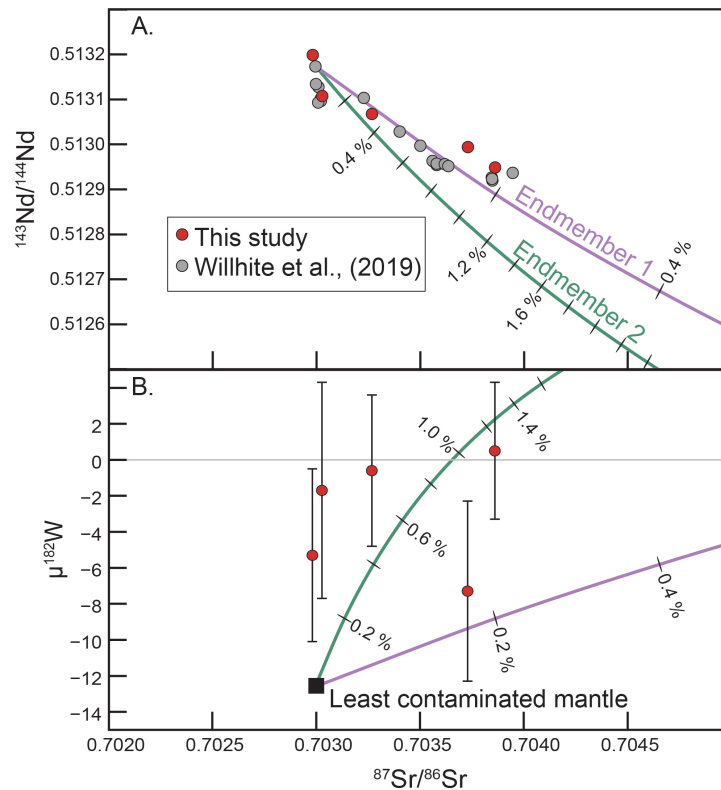


**Figure S-3** Mixing models between uncontaminated mantle and the assumed Precambrian basement of Baffin Island ( $\mu^{182}\text{W} = +20$ ,  $[\text{W}] = 1.9 \mu\text{g g}^{-1}$ ,  $[\text{Sr}] = 192.81 \mu\text{g g}^{-1}$ ,  $[\text{Nd}] = 47.93 \mu\text{g g}^{-1}$ ,  $^{87}\text{Sr}/^{86}\text{Sr} = 0.721081$ ,  $^{143}\text{Nd}/^{144}\text{Nd} = 0.5111164$ ; based on sampled 113450 from Rudnick and Gao, 2003; Larsen and Pedersen, 2009; Willhite *et al.*, 2019). Mixing is strongly dependent on Sr and Nd concentrations in the mantle. Endmember 1 (purple) assumes mantle concentrations ( $[\text{Sr}] = 7.664 \mu\text{g g}^{-1}$ ,  $[\text{Nd}] = 0.581 \mu\text{g g}^{-1}$ ,  $^{87}\text{Sr}/^{86}\text{Sr} = 0.702995$ ,  $^{143}\text{Nd}/^{144}\text{Nd} = 0.513174$ ; Workman and Hart, 2005; Willhite *et al.*, 2019). Partial melting and fractional crystallisation, however, concentrates Sr and Nd in the melt, so endmember 2 provides an upper bound and assumes Sr and Nd concentrations similar to those found in the least contaminated lavas ( $[\text{Sr}] = 48.9 \mu\text{g g}^{-1}$ ,  $[\text{Nd}] = 2.42 \mu\text{g g}^{-1}$ ,  $^{87}\text{Sr}/^{86}\text{Sr} = 0.702995$ ,  $^{143}\text{Nd}/^{144}\text{Nd} = 0.513174$ ; Willhite *et al.*, 2019). Panel (a) shows the radiogenic isotopes of  $^{87}\text{Sr}/^{86}\text{Sr}$  and  $^{143}\text{Nd}/^{144}\text{Nd}$  with these endmembers, and (b) shows how these mixtures effect  $\mu^{182}\text{W}$ . Error bars are 2 s.d., and are smaller than the symbols for Sr and Nd isotopes. Mixing curves have hashes every 0.2 % additional crust.

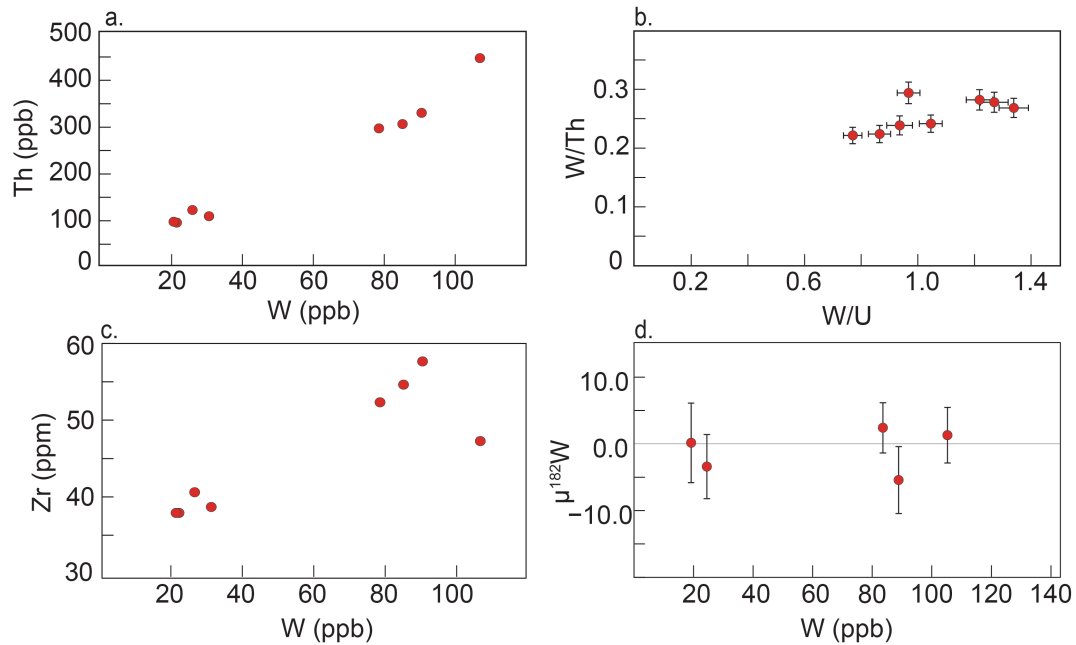


**Figure S-4** Baffin Island  $\mu^{182}\text{W}$  is invariant despite trace element variability. **(a)** Th ( $\text{ng g}^{-1}$ ) versus W concentration ( $\text{ng g}^{-1}$ ). Th and W have similar incompatibilities during igneous differentiation; however, W is more fluid-mobile than Th. The linear trend suggests that the W isotope systematics have not been affected by fluids. Uncertainties are smaller than the symbols. **(b)** W/Th versus W/U. Uranium, Th, and W are similarly incompatible during igneous differentiation, but U is more fluid mobile than W, which is more fluid mobile than Th. Again, fluid enrichment likely did not affect the W concentrations. Error bars reflect 2 s.d. uncertainties associated with W, Th, and U concentration measurements. **(c)** Zr ( $\mu\text{g g}^{-1}$ ) versus W ( $\text{ng g}^{-1}$ ) concentrations. Zr behaves incompatibly during igneous differentiation, so the range in W concentrations is probably the result of igneous differentiation. Uncertainties are smaller than the symbols. **(d)** W concentration ( $\text{ng g}^{-1}$ ) versus  $\mu^{182}\text{W}$ . Error bars are 2 s.e. for the individual analysis.

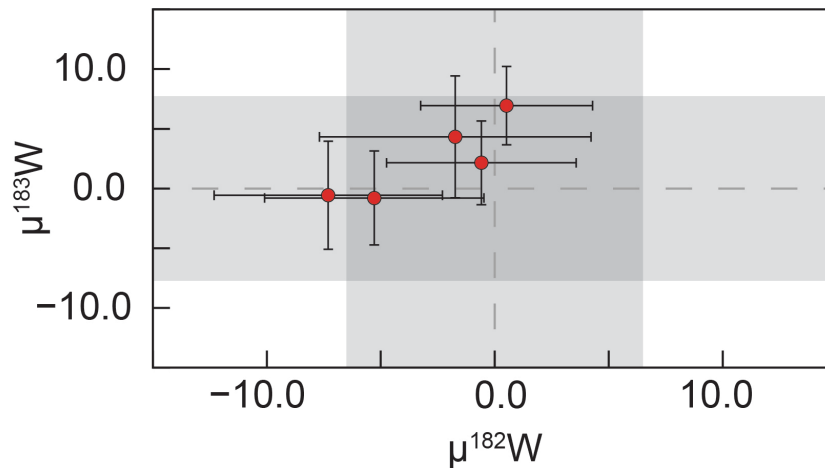


**Figure S-5**  $\mu^{183}\text{W}$  versus  $\mu^{182}\text{W}$  for the five Baffin Island lava samples reported here. Error bars are 2 s.e. for each analysis. Grey regions represent the 2 s.d. of the primary standard, Alfa Aesar.

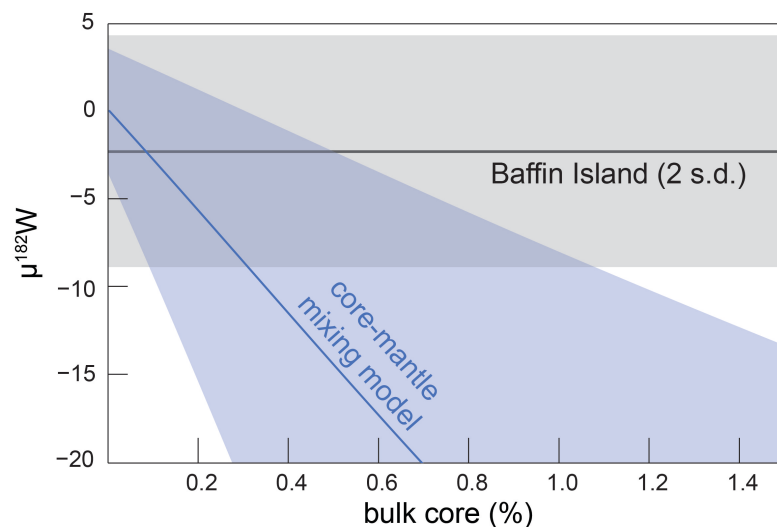


**Figure S-6** Bulk mixing model (blue) between the core ( $\mu^{182}\text{W} = -190 \pm 10$ ,  $500 \pm 120 \text{ ng g}^{-1} \text{ W}$ ; Arevalo and McDonough, 2008; Kleine *et al.*, 2009) and depleted mantle ( $\mu^{182}\text{W} = 0 \pm 3.5$ ,  $29 \text{ ng g}^{-1} \text{ W}$ ; McDonough and Sun, 1995; Rizo *et al.*, 2016; Mundl *et al.*, 2017). The shaded blue region represents the cumulative uncertainty associated with endmember concentrations and isotopic ratios, as well as mass balance. The grey line and shaded region represent the Baffin Island mean ( $-2.29$ , grey line) and 2 s.d. ( $\pm 6.60$ ,  $n = 5$ ), respectively.

## Supplementary Information References

- Archer, G.J., Mundl, A., Walker, R.J., Worsham, E.A., Bermingham, K.R. (2017) High-precision analysis of  $^{182}\text{W}/^{184}\text{W}$  and  $^{183}\text{W}/^{184}\text{W}$  by negative thermal ionization mass spectrometry: Per-integration oxide corrections using measured  $^{18}\text{O}/^{16}\text{O}$ . *International Journal of Mass Spectrometry* 414, 80–86. <https://doi.org/10.1016/j.ijms.2017.01.002>
- Arevalo Jr., R., McDonough, W.F. (2008) Tungsten geochemistry and implications for understanding the Earth's interior. *Earth and Planetary Science Letters* 272, 656–665. <https://doi.org/10.1016/j.epsl.2008.05.031>
- Atreya, S.K., Mahaffy, P.R., Niemann, H.B., Wong, M.H., Owen, T.C. (2003) Composition and origin of the atmosphere of Jupiter—an update, and implications for the extrasolar giant planets. *Planetary and Space Science* 51, 105–112. [https://doi.org/10.1016/S0032-0633\(02\)00144-7](https://doi.org/10.1016/S0032-0633(02)00144-7)
- Breton, T., Quitté, G. (2014) High-precision measurements of tungsten stable isotopes and application to earth sciences. *Journal of Analytical Atomic Spectrometry* 29, 2284–2293. <https://doi.org/10.1039/C4JA00184B>
- Ferrick, A.L., Korenaga, J. (2023) Long-term core–mantle interaction explains W-He isotope heterogeneities. *Proceedings of the National Academy of Sciences* 120, e2215903120. <https://doi.org/10.1073/pnas.2215903120>
- Hart, S.R., Kurz, M.D., Wang, Z. (2008) Scale length of mantle heterogeneities: Constraints from helium diffusion. *Earth and Planetary Science Letters* 269, 508–517. <https://doi.org/10.1016/j.epsl.2008.03.010>
- Horton, F., Asimow, P.D., Farley, K.A., Curtice, J., Kurz, M.D., Blusztajn, J., Biasi, J., Boyes, X.M. (2023) Highest terrestrial  $^3\text{He}/^4\text{He}$  credibly from the core. *Nature* 623, 90–94. <https://doi.org/10.1038/s41586-023-06590-8>
- Kleine, T., Touboul, M., Bourdon, B., Nimmo, F., Mezger, K., Palme, H., Jacobsen, S.B., Yin, Q.-Z., Halliday, A.N. (2009) Hf–W chronology of the accretion and early evolution of asteroids and terrestrial planets. *Geochimica et Cosmochimica Acta* 73, 5150–5188. <https://doi.org/10.1016/j.gca.2008.11.047>
- Kruijer, T.S., Kleine, T. (2018) No  $^{182}\text{W}$  excess in the Ontong Java Plateau source. *Chemical Geology* 485, 24–31. <https://doi.org/10.1016/j.chemgeo.2018.03.024>
- Kruijer, T.S., Sprung, P., Kleine, T., Leya, I., Burkhardt, C., Wieler, R. (2012) Hf–W chronometry of core formation in planetesimals inferred from weakly irradiated iron meteorites. *Geochimica et Cosmochimica Acta* 99, 287–304. <https://doi.org/10.1016/j.gca.2012.09.015>
- Larsen, L.M., Pedersen, A.K. (2009) Petrology of the Paleocene Picrites and Flood Basalts on Disko and Nuussuaq, West Greenland. *Journal of Petrology* 50, 1667–1711. <https://doi.org/10.1093/petrology/egp048>
- McDonough, W.F., Sun, S.-s. (1995) The composition of the Earth. *Chemical Geology* 120, 223–253. [https://doi.org/10.1016/0009-2541\(94\)00140-4](https://doi.org/10.1016/0009-2541(94)00140-4)
- Moreira, M.A., Kurz, M.D. (2013) Noble Gases as Tracers of Mantle Processes and Magmatic Degassing. In: Burnard, P. (Ed.) *The Noble Gases as Geochemical Tracers*. Advances in Isotope Geochemistry, Springer, Berlin, Heidelberg, 371–391. [https://doi.org/10.1007/978-3-642-28836-4\\_12](https://doi.org/10.1007/978-3-642-28836-4_12)
- Mundl, A., Touboul, M., Jackson, M.G., Day, J.M.D., Kurz, M.D., Lekic, V., Helz, R.T., Walker, R.J. (2017) Tungsten-182 heterogeneity in modern ocean island basalts. *Science* 356, 66–69. <https://doi.org/10.1126/science.aal4179>
- Mundl-Petermeier, A., Walker, R.J., Jackson, M.G., Blichert-Toft, J., Kurz, M.D., Halldórsson, S.A. (2019) Temporal evolution of primordial tungsten-182 and  $^3\text{He}/^4\text{He}$  signatures in the Iceland mantle plume. *Chemical Geology* 525, 245–259. <https://doi.org/10.1016/j.chemgeo.2019.07.026>



- Mundl-Petermeier, A., Walker, R.J., Fischer, R.A., Lekic, V., Jackson, M.G., Kurz, M.D. (2020) Anomalous  $^{182}\text{W}$  in high  $^3\text{He}/^4\text{He}$  ocean island basalts: Fingerprints of Earth's core? *Geochimica et Cosmochimica Acta* 271, 194–211. <https://doi.org/10.1016/j.gca.2019.12.020>
- Nagai, Y., Yokoyama, T. (2014) Chemical Separation of Mo and W from Terrestrial and Extraterrestrial Samples via Anion Exchange Chromatography. *Analytical Chemistry* 86, 4856–4863. <https://doi.org/10.1021/ac404223t>
- Nakanishi, N., Puchtel, I.S., Walker, R.J., Nabelek, P.I. (2023) Dissipation of Tungsten-182 Anomalies in the Archean Upper Mantle: Evidence from the Black Hills, South Dakota, USA. *Chemical Geology* 617, 121255. <https://doi.org/10.1016/j.chemgeo.2022.121255>
- Reimink, J.R., Mundl-Petermeier, A., Carlson, R.W., Shirey, S.B., Walker, R.J., Pearson, D.G. (2020) Tungsten Isotope Composition of Archean Crustal Reservoirs and Implications for Terrestrial  $\mu^{182}\text{W}$  Evolution. *Geochemistry, Geophysics, Geosystems* 21, e2020GC009155. <https://doi.org/10.1029/2020GC009155>
- Rizo, H., Walker, R.J., Carlson, R.W., Horan, M.F., Mukhopadhyay, S., Manthos, V., Francis, D., Jackson, M.G. (2016) Preservation of Earth-forming events in the tungsten isotopic composition of modern flood basalts. *Science* 352, 809–812. <https://doi.org/10.1126/science.aad8563>
- Rizo, H., Andraut, D., Bennett, N.R., Humayun, M., Brandon, A., Vlastelic, I., Moine, B., Poirier, A., Bouhifd, M.A., Murphy, D.T. (2019)  $^{182}\text{W}$  evidence for core-mantle interaction in the source of mantle plumes. *Geochemical Perspectives Letters* 11, 6–11. <https://doi.org/10.7185/geochemlet.1917>
- Rudnick, R.L., Gao, S. (2003) 3.01 - Composition of the Continental Crust. In: Holland, H.D., Turekian, K.K. (Eds.) *Treatise on Geochemistry*. First Edition, Elsevier, Amsterdam, 1–64. <https://doi.org/10.1016/B0-08-043751-6/03016-4>
- St-Onge, M.R., Van Gool, J.A.M., Garde, A.A., Scott, D.J. (2009) Correlation of Archean and Palaeoproterozoic units between northeastern Canada and western Greenland: constraining the pre-collisional upper plate accretionary history of the Trans-Hudson orogen. In: Cawood, P.A., Kröner, A. (Eds.) *Earth Accretionary Systems in Space and Time*. Geological Society of London, London, 193–236. <https://doi.org/10.1144/sp318.7>
- St-Onge, M.R., Scott, D.J., Rayner, N., Sanborn-Barrie, M., Skipton, D.R., Saumur, B.M., Wodicka, N., Weller, O.M. (2020) Archean and Paleoproterozoic cratonic rocks of Baffin Island. In: Dafoe, L.T., Bingham-Koslowski, N. (Eds.) *Geological Survey of Canada, Bulletin 608*. Geological Survey of Canada, Montreal, 25–53. <https://doi.org/10.4095/321824>
- Touboul, M., Walker, R.J. (2012) High precision tungsten isotope measurement by thermal ionization mass spectrometry. *International Journal of Mass Spectrometry* 309, 109–117. <https://doi.org/10.1016/j.ijms.2011.08.033>
- Völkening, J., Köppe, M., Heumann, K.G. (1991) Tungsten isotope ratio determinations by negative thermal ionization mass spectrometry. *International Journal of Mass Spectrometry and Ion Processes* 107, 361–368. [https://doi.org/10.1016/0168-1176\(91\)80070-4](https://doi.org/10.1016/0168-1176(91)80070-4)
- Willhite, L.N., Jackson, M.G., Blichert-Toft, J., Bindeman, I., Kurz, M.D., Halldórsson, S.A., Harðardóttir, S., Gazel, E., Price, A.A., Byerly, B.L. (2019) Hot and Heterogenous High- $^3\text{He}/^4\text{He}$  Components: New Constraints From Proto-Iceland Plume Lavas From Baffin Island. *Geochemistry, Geophysics, Geosystems* 20, 5939–5967. <https://doi.org/10.1029/2019GC008654>
- Workman, R.K., Hart, S.R. (2005) Major and trace element composition of the depleted MORB mantle (DMM). *Earth and Planetary Science Letters* 231, 53–72. <https://doi.org/10.1016/j.epsl.2004.12.005>
- Yoshino, T., Makino, Y., Suzuki, T., Hirata, T. (2020) Grain boundary diffusion of W in lower mantle phase with implications for isotopic heterogeneity in oceanic island basalts by core-mantle interactions. *Earth and Planetary Science Letters* 530, 115887. <https://doi.org/10.1016/j.epsl.2019.115887>

